Robust Infrared Small Target Detection Using a Novel Four-Leaf Model

Dali Zhou and Xiaodong Wang

***Abstract*—Infrared small target detection is widely used in the military field, and robust infrared small target detection has significant significance. Inspired by plants, an infrared small target detection method based on the four-leaf model is proposed. This model has both macro and micro attributes, with macro attributes referred to as the background suppressor (BS) and micro attributes referred to as the texture collector (TC). BS is a four-neighborhood model that can achieve background suppression while reducing the interference of bright background clutter in the target neighborhood to a certain extent. TC can collect texture information of small targets and improve the enhancement effect of small targets. The fusion of TC and BS can effectively suppress background clutter and improve the detection performance of infrared small targets. The experiment is carried out on five real infrared image sequences. The results show that the proposed infrared small target detection method can improve the detection rate and reduce the false alarm rate in the face of infrared images with complex backgrounds. Compared to existing algorithms, the algorithm has high robustness.**

***Index Terms*—Background suppressor (BS), detection rate, false alarm rate, infrared small target detection, texture collector (TC).**

I. Introduction

SMALL target detection is an important technology in infrared search and tracking systems [1], [2]. Infrared target detection is widely used in the military field, which can warn enemy aircraft and helicopters [3], [4], [5], [6], [7], and is one of the most important technologies in the passive defense system [8], [9], [10]. Due to the long imaging distance, the target is dark and small, and there is no fixed information about shape, texture, and structure [11]. And the target is usually immersed in a complex background [12]. Infrared small targets with few effective pixels and background clutter exhibit similar characteristics. Even in some complex backgrounds, it is difficult for the naked eye to recognize small infrared targets from a single frame image. Therefore, improving the detection performance of infrared small targets in complex backgrounds is still a difficult task.

Traditional small target detection methods are some basic filters, such as maximum mean/maximum median filter [13], top hat filter [14], two-dimensional least mean square adaptive filter [15], etc. However, these methods will degrade the detection performance and have a serious false alarm rate when the SCR is low. There are also methods based on low-rank matrix recovery, such as the infrared patch-image model [16], the robust principal component analysis [17], the stable multi subspace learning [18], reweighted infrared patch tensor model [19], and nonconvex rank approximation minimization [20]. In recent years, people have done important research on detection methods based on human vision system (HVS). These methods focus on the contrast and difference between the target and its surrounding background. Chen et al. [21] proposed a local contrast measure (LCM) algorithm, which uses an image patch to divide the surrounding parts into eight directions to suppress the background. Wei et al. [22] proposed a multiscale patch-based contrast measure (MPCM). Bai and Bi [23] proposed a derivative entropy contrast measure and Deng et al. [24] proposed a weighted local difference measure. These algorithms utilize the local contrast difference of small targets to achieve target enhancement and background suppression. Therefore, these methods are sensitive to highlight background and background clutter [25]. When the infrared image background is complex, the stability performance of the algorithm is poor. Shi et al. [26] proposed a high-boost-based multiscale local contrast measure for the small target detection in the complex backgrounds. Han et al. [27] proposed a multiscale tri-layer local contrast measure. Nasiri and Chehresa [30] proposed a novel three-layer patch-image model, where the variance difference is weighted between each part. Tang et al. [32] proposed a high-performance detection method with fast processing speed and detection effectiveness by global contrast measure (GCM). Faced with different complex and ever-changing infrared image sequences, these algorithms find it difficult to maintain superior detection performance. These algorithms are greatly affected by the bright background clutter in the target neighborhood.

To improve the robustness of the algorithm, we propose a four-leaf model inspired by plants. This model has both macro and microscopic properties, namely the background suppressor and texture collector in the model. Background suppressor mainly achieves complex background elimination, while texture collector achieves feature extraction of infrared small targets in complex backgrounds. With this algorithm structure, the four-leaf model ingeniously separates the background suppression function from the target enhancement function. Compared with the traditional method, the four-leaf model is more consistent with the characteristics of infrared small targets, so it has higher target recognition accuracy. In addition, using four adjacent

Manuscript received 8 September 2023; revised 3 October 2023 and 2 November 2023; accepted 23 November 2023. Date of publication 30 November 2023; date of current version 14 December 2023. This work was supported by the Strategic Priority Research Program of Chinese Academy of Sciences under Grant XDA17010205. *(Corresponding author: Dali Zhou.)*

The authors are with the Changchun Institute of Optics, Fine Mechanics and Physics, Chinese Academy of Sciences, Changchun 130033, China (e-mail: 695344479@qq.com; wangxd@ciomp.ac.cn).

Digital Object Identifier 10.1109/JSTARS.2023.3337996

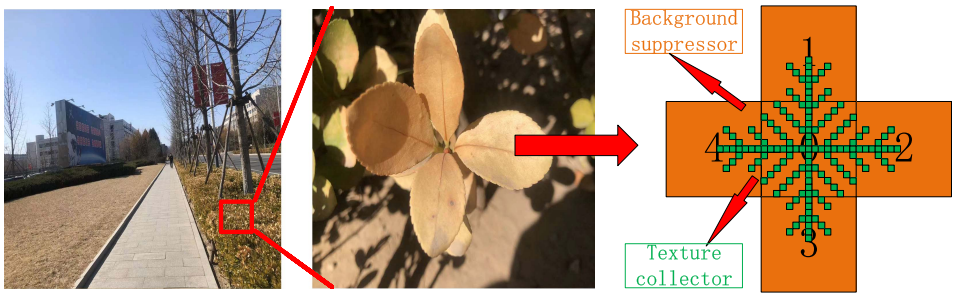

Fig. 1. Four-leaf model inspired by plant.

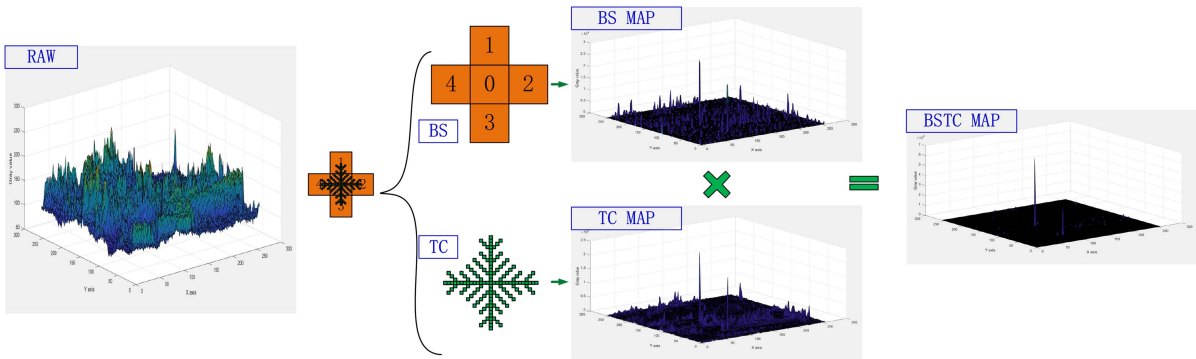

Fig. 2. Flowchart of the proposed algorithm.

regions that are relatively close to the target for local contrast calculation can effectively suppress the interference of bright background clutter in the target neighborhood in some complex image sequences and improve the detection performance of small infrared targets in complex backgrounds. We analyzed the principle and feasibility of the algorithm in detail. The experimental results show that the proposed method in this article has certain advantages.

II. Proposed Algorithm

Fig. 1 is the four-leaf model inspired by plants. This model consists of two parts: one is the background suppressor composed of four leaves, abbreviated as BS, and the other is the texture collector composed of leaf textures, abbreviated as TC. The flowchart of the algorithm is shown in Fig. 2. We use a four-leaf model to achieve background suppression and target enhancement, thereby extracting targets. Specifically, BS achieves background cancellation, while TC is responsible for extracting target features. Independent design of two functions will help improve background noise suppression. Then, the BS map and the TC map are fused to obtain the BSTC map. After image fusion, the background is significantly suppressed and the target is significantly enhanced. Finally, the adaptive threshold method is used to obtain the infrared small target.

A. BSTC Calculation

We used the four-leaf model for local contrast measure, as shown in Fig. 3. In the traditional nine-cell model when there is background clutter around a small target, it will participate in the calculation. According to the theory of local contrast computation, this will affect the enhancement effect of small targets, as shown in Fig. 3(c), thus affecting the detection rate. Then, adopting an adaptive threshold segmentation algorithm to detect targets will result in a higher false alarm rate in order to achieve a higher detection probability. Different from the traditional nine-cell model, our four-leaf model uses four neighborhoods in the calculation to eliminate the background, which can suppress the interference of the highlight background, and the highlight background clutter in the target neighborhood to a certain extent, as shown in Fig. 3(e). Therefore, compared with the nine-cell model, the four-leaf model has a certain high robustness.

First, inspired by the LCM algorithm [21] and RLCM algorithm [28], BS is implemented using the following:

$$\mathrm{BS} = \mathrm{MAX}\left\{\mathrm{IT}_0 * (\mathrm{IT}_0 - \mathrm{IB}), 0\right\} \tag{1}$$

where IT_0 represents the gray value of the target, IB represents the gray value of the background, which are calculated as follows:

$$\mathrm{IT}_0 = \frac{1}{N1}\sum_{K=1}^{N1} I_0^K \tag{2}$$

$$\begin{aligned}\mathrm{IB} &= \mathrm{MAX}\left\{\mathrm{IB}_i \,|i = 1, 2, 3, 4\right\} \\ &= \mathrm{MAX}\left\{\frac{1}{N2}\sum_{K=1}^{N2} I_i^K \,|i = 1, 2, 3, 4\right\}\end{aligned} \tag{3}$$

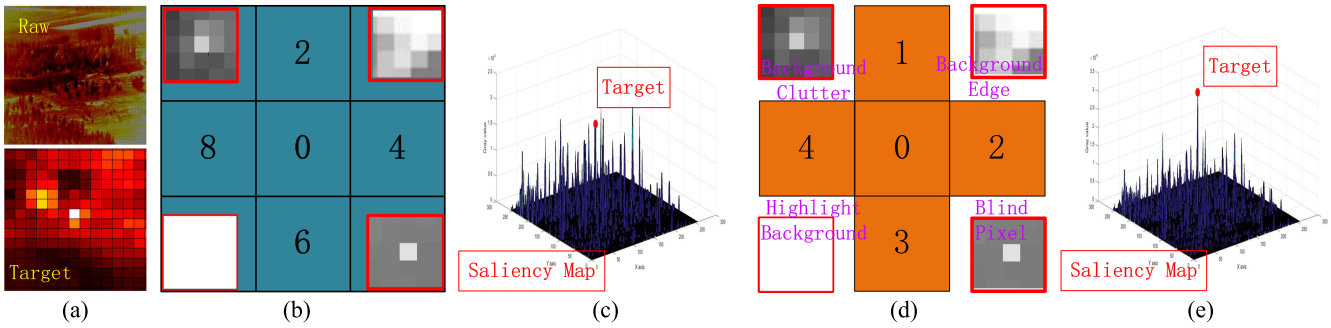

Fig. 3. (a) Raw image. (b) Traditional nine-cell model. (c) Saliency map obtained by the nine-cell model. (d) Four-leaf model. (e) Saliency map obtained by the four-leaf model.

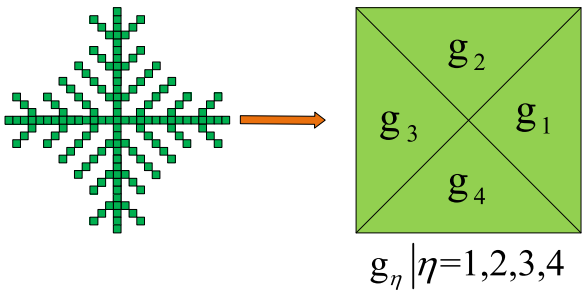

Fig. 4. Texture collector (TC).

where I_0^K is the Kth maximal gray value in cell(0), I_i^K is the Kth maximal gray value in cell$(i)|i = 1, 2, 3, 4$, and $N1$ and $N2$ represent the numbers of maximal gray values considered.

Second, the image gradient is used to achieve the function of TC. Given a raw image, the infrared gradient vector field can be calculated as follows [33]:

$$\nabla f(x,y) = \left[f'_x(x,y) f'_y(x,y)\right]^T \tag{4}$$

$$f'_x(x,y) = \frac{f(x+1,y) - f(x-1,y)}{2} \tag{5}$$

$$f'_y(x,y) = \frac{f(x,y+1) - f(x,y-1)}{2} \tag{6}$$

where $f'_x(x,y)$ and $f'_y(x,y)$ are the gradient values in the x-direction and y-direction, respectively. This article defines the four-direction gradient as follows:

$$G_\eta(i,j) = \begin{cases} \mathrm{MAX}\left\{I(i,j-1) - I(i,j), 0\right\}, \eta = 1 \\ \mathrm{MAX}\left\{I(i+1,j) - I(i,j), 0\right\}, \eta = 2 \\ \mathrm{MAX}\left\{I(i,j+1) - I(i,j), 0\right\}, \eta = 3 \\ \mathrm{MAX}\left\{I(i-1,j) - I(i,j), 0\right\}, \eta = 4. \end{cases} \tag{7}$$

Then, we divided TC into four regions, as shown in Fig. 4. Four regions correspond to four directions, and a gradient set for each region is constructed by calculating the gradients of all pixels in the corresponding direction in each region. The set of gradients in four regions is represented by the following:

$$gr_\eta(i,j) = \left\{G_\eta(i+m, j+n) \,|(i+m, j+n) \in \mathrm{g}_\eta\right\}, \eta = 1,2,3,4 \tag{8}$$

where $g_\eta|\eta = 1,2,3,4$ represents the four regions of the TC, (i,j) represents the current coordinate of the center of the TC, and. $(i+m, j+n)$ represents the pixel coordinate in the four regions. The mean square value of a region is calculated using the following:

$$\begin{aligned} \mathrm{aveg}_\eta(i,j) &= \frac{\mathrm{SUM}\left(gr_\eta^2(i,j)\right)}{\mathrm{MAX}\left\{\|gr_\eta\|_0, 1\right\}}, \eta = 1,2,3,4 \\ &= \frac{\mathrm{SUM}\left(\left\{G_\eta^2(i+m, j+n) \,|(i+m, j+n) \in \mathrm{g}_\eta\right\}\right)}{\mathrm{MAX}\left\{\|gr_\eta\|_0, 1\right\}}, \eta = 1,2,3,4 \end{aligned} \tag{9}$$

where $\| \bullet \|_0$ represents the number of nonzero elements. Then, TC function can be achieved as follows:

$$\mathrm{TC} = \sum_{\eta=1}^{4} \mathrm{aveg}_\eta = \sum_{\eta=1}^{4} \frac{\mathrm{SUM}\left(gr_\eta^2\right)}{\mathrm{MAX}\left\{\|gr_\eta\|_0, 1\right\}}. \tag{10}$$

Finally, we get the calculation method of the four-leaf model, as shown in (11). It can be easily seen that after processing by BS, the parts of the image that are less than 0 are no longer involved in subsequent calculations. Therefore, multiplying with TC can obtain higher precision target feature extraction results

$$\begin{aligned} \mathrm{BSTC} &= \mathrm{BS} * \mathrm{TC} \\ &= \mathrm{MAX}\left\{\mathrm{IT}_0 * (\mathrm{IT}_0 - \mathrm{IB}), 0\right\} * \sum_{\eta=1}^{4} \frac{\mathrm{SUM}\left(gr_\eta^2\right)}{\mathrm{MAX}\left\{\|gr_\eta\|_0, 1\right\}}. \end{aligned} \tag{11}$$

In some complex infrared image sequences with complex backgrounds, the four-leaf model has better detection performance. We conducted comparative experiments on four real infrared image sequences. In the experiment, we only use BS to detect infrared small targets in four-leaf and nine-cell modes, respectively. Fig. 5 shows the influence of the proposed four-leaf model and the traditional nine-cell model on the detection performance of small infrared targets. It can be seen that in some complex infrared sequence images, due to the reduction of the calculation area, the four-leaf model can reduce the interference of the background clutter to a certain extent and improve the detection performance of small infrared targets.

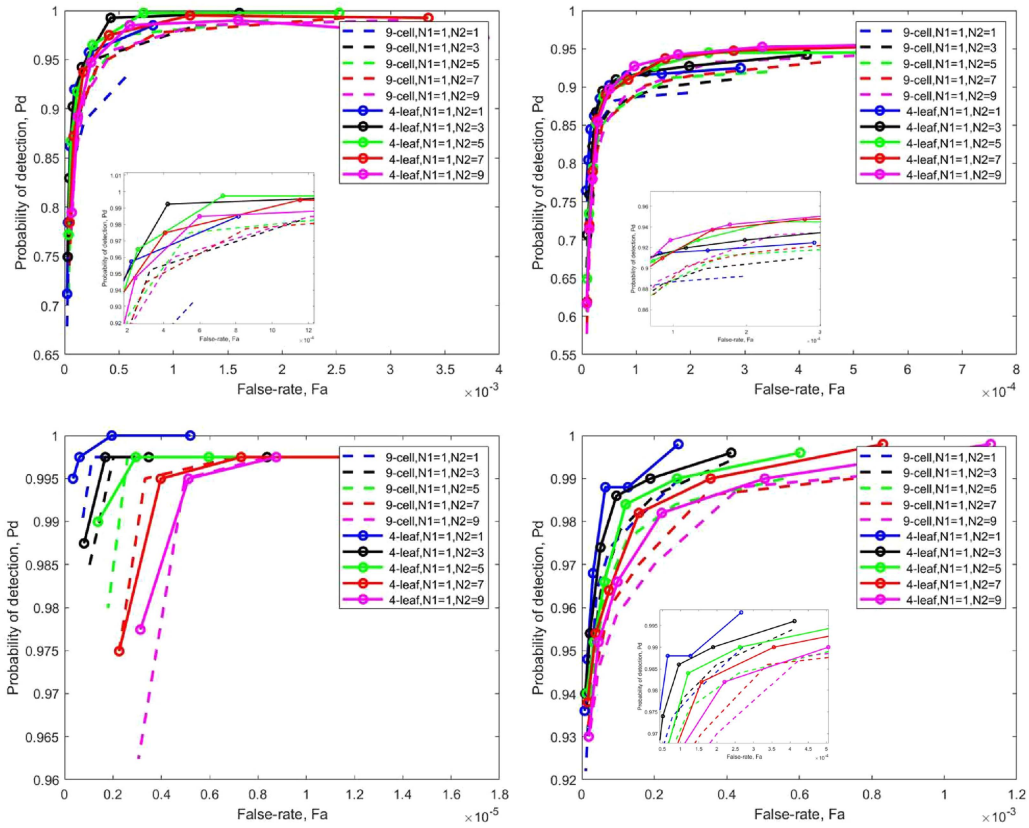

Fig. 5. Comparison of detection performance between four-leaf and nine-cell model.

B. About Parameter Selection

About the background suppressor, the two parameters $N1$ and $N2$ are adjustable, which can increase the flexibility and adaptability of the algorithm. This is also a key factor in the algorithm's high detection performance. Therefore, it is necessary to explain the two-parameter settings of the algorithm. We conducted experiments on four real infrared image sequences.

In Fig. 6, the target size of Seq. 1 is less than $3 * 3$ pixels, and the number of effective pixels is between 1 and 2 pixels. It can be seen that when N2 is fixed, the more N1 deviates from the number of effective pixels, the worse the detection performance. In Seq. 2, the target size ranges from $3 * 3$ pixels to $5 * 5$ pixels, and the effective number of pixels is about 5 to 13 pixels. When N2 is fixed, the greater the deviation of N1 from the effective pixels, the worse the detection performance. In Seq. 3, the target size is less than $3 * 3$ pixels, and the effective number of pixels is about 1 to 2 in most images. When N2 is fixed, the greater the deviation of N1 from the effective pixels, the worse the detection performance. In Seq. 4, the target size is less than $3 * 3$ pixels, and the effective number of pixels is about 1 to 4 pixels. When N2 is fixed, the greater the deviation of N1 from the effective pixels, the worse the detection performance. In our experiment, N1 should be similar to the effective number of pixels of the target. From the four experiments, it can be seen that when N1 is fixed, N2 does not significantly affect the detection probability, but has a certain impact on the false alarm rate. We suggest that N1 should be similar to the effective number of pixels of the target, and N2 can be finetuned according to the specific infrared image sequence to reduce the false alarm rate.

Regarding the texture collector, it is recommended that the size should fully include the target area to complete the full target texture collection. In the face of complex image sequences, it can be adjusted appropriately to improve the accuracy of texture collection.

C. Threshold Segmentation Algorithm

Equation (12) is used for threshold segmentation. Considering part background of the saliency map becomes zero, so we use the mean value of removing zero here

$$\mathrm{Th} = k \times I_{\max} + (1 - k) \times I_{\mathrm{mean}(\sim 0)} \tag{12}$$

where $I_{\max}$ is the maximum gray value of the saliency map, $I_{\mathrm{mean}(\sim 0)}$ is the mean value excluding zero, and k is a threshold coefficient between 0 and 1.

III. Simulations and Experimental Results

In order to verify the effectiveness of the algorithm, five real infrared sequences [34] are used. The detailed information of infrared small target image sequences is shown in Table I.

We compare six algorithms, including RLCM [28], WSLCM [29], MPCM [22], VARD [30], TTLDM [31], and GCM [32].

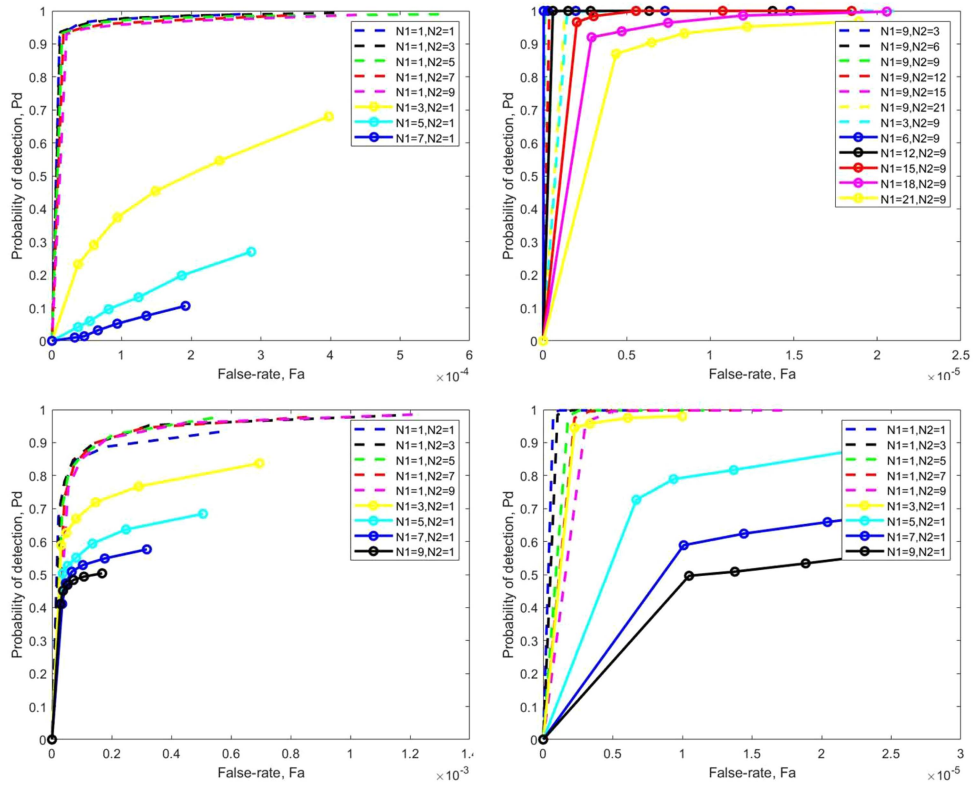

Fig. 6. Influence of parameters.

TABLE I
DETAILS OF THE IR SEQUENCES

	Frames	Size	Target number	Target size	Target Type
Seq.1	399	256*256	1	2*2 to 3*3	Plane
Seq.2	399	256*256	1	3*3 to 5*5	Plane
Seq.3	399	256*256	1	2*2 to 3*3	Plane
Seq.4	399	256*256	1	3*3 to 5*5	Plane
Seq.5	500	256*256	1	2*2 to 3*3	Plane

Fig. 7 shows the processing results of different algorithms for a single image. We can see that in the original infrared image sequences, the background is complex. There are bright backgrounds, complex background edges, and background clutter. TTLDM uses a trilayer template for local difference measure which combines the grayscale difference and grayscale variance. This method has good background suppression performance but is susceptible to interference from bright background clutter. The RCLM algorithm leaves behind a lot of background clutter. WSLCM and MPCM are improved algorithms based on LCM. They can remove background information well, but the target is still interfered with background clutter. The VARD algorithm has a strong background suppression ability. The calculation of variance will significantly enhance some bright background clutter, causing some targets to be submerged. GCM is the latest high-performance algorithm with high efficiency. However, due to the limited number of pixels involved in contrast calculation, a certain amount of background clutter remains in the saliency map. At the same time, the enhancement effect for large targets is poor in some complex scenes. Overall, these algorithms are interfered with background clutter to varying degrees. Compared to these algorithms, our algorithm achieves the best background suppression and target enhancement effects, and the saliency maps are very clean.

The processing effect of a single image roughly reflects the background suppression ability and target enhancement effect of the algorithm. To further illustrate the advantages of this algorithm, the receiver operating characteristic (ROC) curves of different algorithms are also shown in Fig. 8. The ROC curve can well reflect the detection performance and robustness of the algorithm. Overall, our algorithm has the best ROC curve, indicating that our algorithm has achieved the best detection performance among these five sequences with high robustness. From the five ROC curves, it can be seen that the robustness of MPCM, VARD, and TLLDM is poor in some complex scenes. These algorithms are susceptible to the influence of bright background clutter, which can affect detection performance. The WSLCM algorithm does not achieve good detection performance in these five sequences and it has poor detection performance when dealing with infrared image sequences of weak and small targets in some complex scenes. The pixels involved in RLCM calculation are adjustable, which increases the adaptability to different scenes. However, this algorithm only calculates local contrast, which leads to certain bottlenecks in the detection performance of the algorithm. The GCM algorithm is the latest proposed infrared small target detection

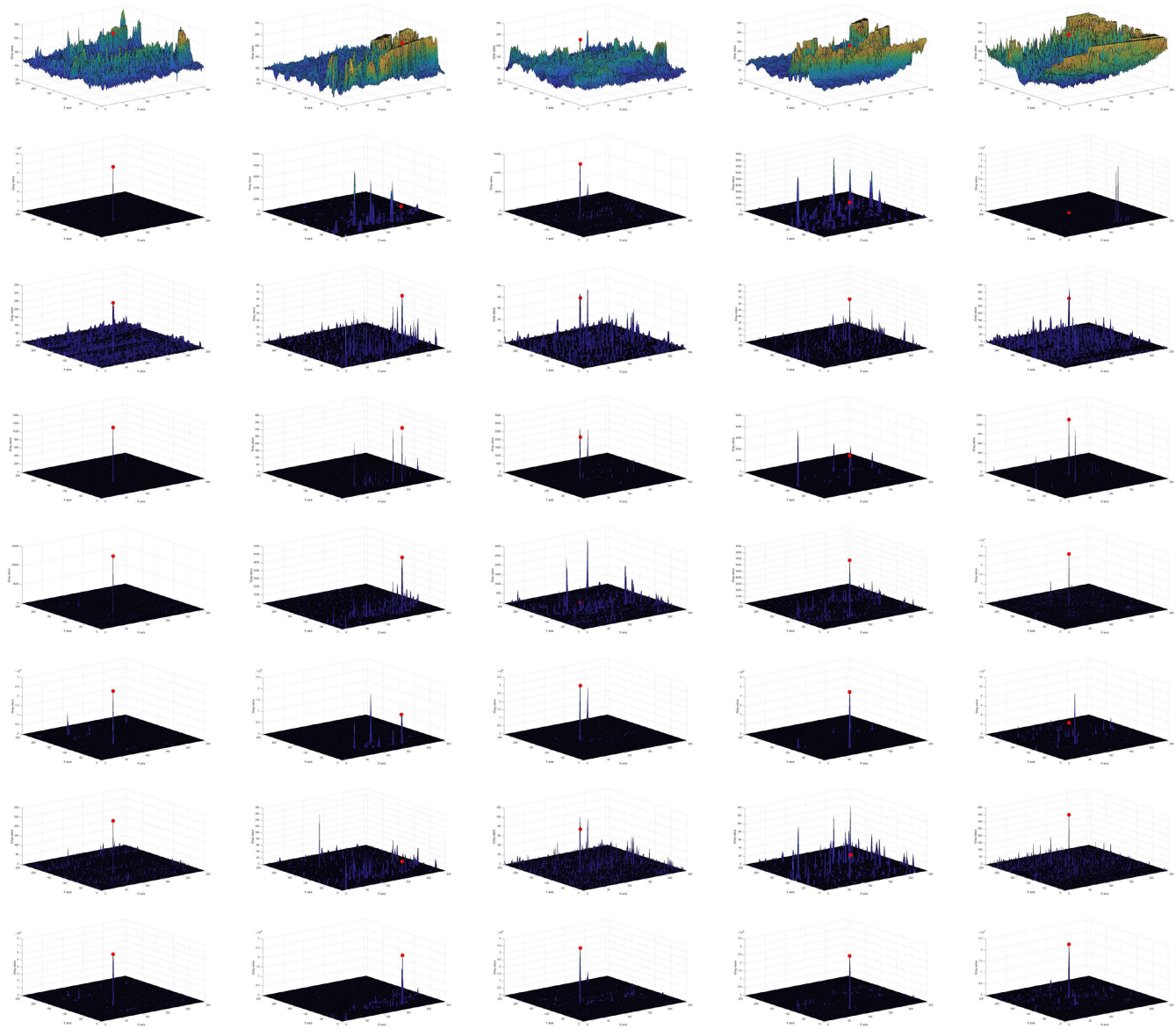

Fig. 7. From (left to right): Seq. 1–Seq. 5. From (top to bottom): Raw images, TTLDM results, RLCM results, WSLCM results, MPCM results, VARD results, GCM results, BSTC results.

algorithm, which has the characteristics of high performance and fast speed. Compared with other algorithms, it performs relatively well for some small-sized targets. However, due to the dilation operation of morphology, it outputs the maximum pixel as the background gray value, which to some extent limits the performance of the algorithm. Therefore, for Seq. 2 and Seq. 4, the detection performance severely decreases in complex backgrounds with relatively large target sizes. The algorithm proposed in this article has the best performance. Compared with other algorithms, it has higher robustness in the detection of small infrared targets in different scenes with different features. Compared with these algorithms, the four-leaf model is considered more comprehensively. The calculation methods of BS and TC in macro and micro aspects have achieved higher accuracy in small target recognition. A highly robust BS can effectively suppress the interference of bright background clutter in the target neighborhood. A high-precision TC specifically extracts infrared small target features. The fusion of BS and TC can effectively suppress background clutter and improve target saliency. The processing effect of a single image proves that the algorithm has both a high-precision background cancellation effect and a high stability target enhancement effect. The ROC curves of image sequences further prove that the algorithm has high robustness and high target detection probability.

In addition, we use Seq. 5 in Table I as a reference to calculate the calculation time of different algorithms, as shown in Table II.

TABLE II
CALCULATION TIME OF DIFFERENT METHODS

TLLDM	RLCM	WSLCM	MPCM	VARD	GCM	PRO
0.0115	0.2088	0.1655	0.0151	0.0120	0.0053	0.2770

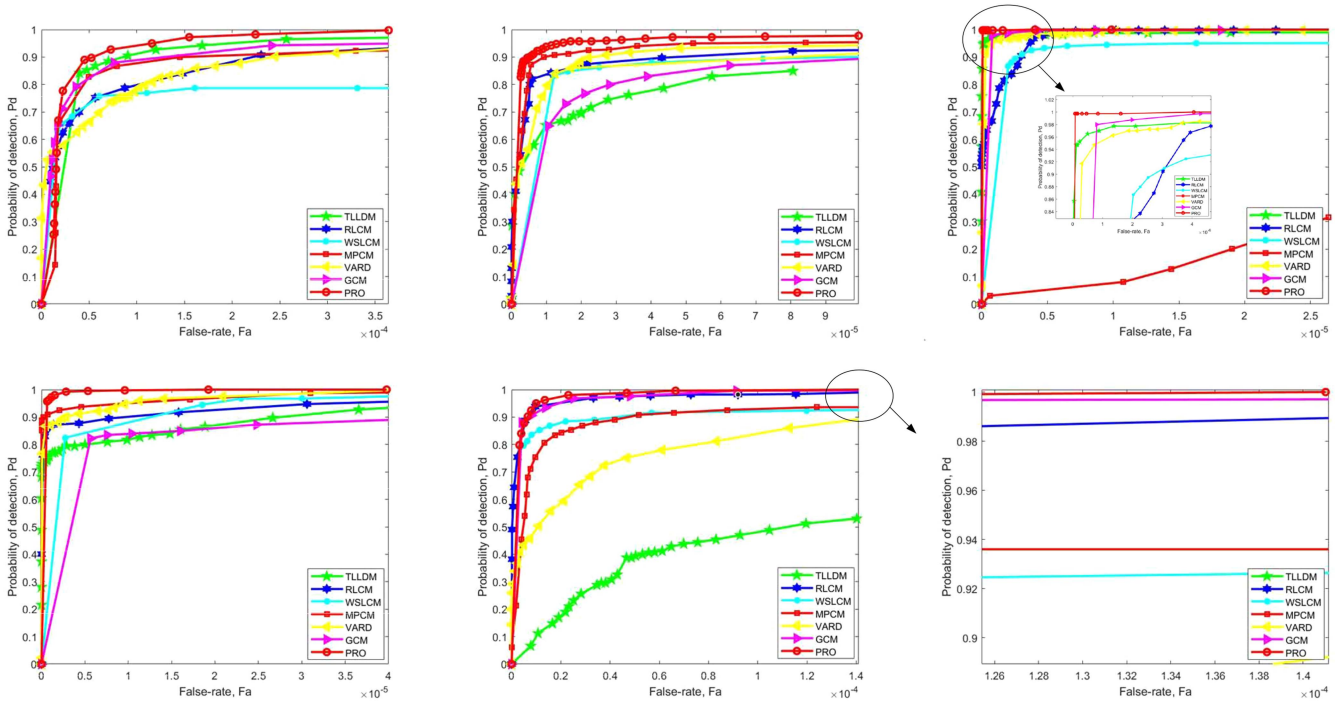

Fig. 8. ROC curves of Seq. 1–Seq. 5.

Compared to the other six algorithms, our algorithm requires slightly more time. That is to say, we achieve high detection performance and high robustness by sacrificing some calculation time. This is also the shortcoming of the algorithm proposed in this article.

IV. Conclusion

Inspired by plants, a highly robust infrared small target detection method is proposed, which is called the four-leaf model. In the article, the leaf part of the four-leaf model achieves a high robustness background suppression function. We use four neighboring regions close to targets for background cancellation, which to some extent reduces the interference of bright background clutter in the target neighborhood. The texture of the four-leaf model is designed as a texture collector, which accurately extracts target features and achieves target enhancement. Experiments are conducted on five image sequences and six algorithms are compared. The experimental results show that the four-leaf model inspired by plants has high target recognition accuracy and is a robust infrared small target detection method.

References

[1] S. Kim and J. Lee, "Scale invariant small target detection by optimizing signal-to-clutter ratio in heterogeneous background for infrared search and track," *Pattern Recognit.*, vol. 45, no. 1, pp. 393–406, 2012.

[2] X. Bai, Z. Chen, Y. Zhang, Z. Liu, and Y. Lu, "Infrared ship target segmentation based on spatial information improved FCM," *IEEE Trans. Cybern.*, vol. 46, no. 12, pp. 3259–3271, Dec. 2016.

[3] J. Du et al., "A spatial-temporal feature-based detection framework for infrared dim small target," *IEEE Trans. Geosci. Remote Sens.*, vol. 60, 2022, Art. no. 3000412.

[4] J. Zhao et al., "Infrared small target detection using sparse representation," *J. Syst. Eng. Electron.*, vol. 22, no. 6, pp. 897–904, 2011.

[5] R. Liu et al., "Infrared point target detection with improved template matching," *Infrared Phys. Technol.*, vol. 55, no. 4, pp. 380–387, 2012.

[6] T. W. Bae, "Small target detection using bilateral filter and temporal cross product in infrared images," *Infrared Phys. Technol.*, vol. 54, no. 5, pp. 403–411, 2011.

[7] G. Wang et al., "Efficient small-target detection algorithm," in *Proc. 4th Signal Process., Sensor Fusion, Target Recognit.*, 1995, pp. 321–329.

[8] L. Wu, Y. Ma, F. Fan, M. Wu, and J. Huang, "A double-neighborhood gradient method for infrared small target detection," *IEEE Geosci. Remote Sens. Lett.*, vol. 18, no. 8, pp. 1476–1480, Aug. 2021.

[9] C. Yang et al., "Directional support value of Gaussian transformation for infrared small target detection," *Appl. Opt.*, vol. 54, no. 9, pp. 2255–2265, 2015.

[10] A. Dehghani and A. Parsayan, "Small target detection and tracking based on the background elimination and Kalman filter," in *Proc. Int. Symp. Artif. Intell. Signal Process.*, 2015, pp. 328–333.

[11] D. Zhou and X. Wang, "Research on high robust infrared small target detection method in complex background," *IEEE Geosci. Remote Sens. Lett.*, vol. 20, 2023, Art. no. 6007705.

[12] J. Han, Y. Ma, J. Huang, X. Mei, and J. Ma, "An infrared small target detecting algorithm based on human visual system," *IEEE Geosci. Remote Sens. Lett.*, vol. 13, no. 3, pp. 452–456, Mar. 2016.

[13] S. D. Deshpande et al., "Max-mean and max-median filters for detection of small targets," in *Proc. Signal Data Process. Small Targets*, 1999, pp. 74–83.

[14] X. Bai and F. Zhou, "Analysis of new top-hat transformation and the application for infrared dim small target detection," *Pattern Recognit.*, vol. 43, no. 6, pp. 2145–2156, 2010.

[15] T. Soni, J. R. Zeidler, and W. H. Ku, "Performance evaluation of 2-D adaptive prediction filters for detection of small objects in image data," *IEEE Trans. Image Process.*, vol. 2, no. 3, pp. 327–340, Jul. 1993.

[16] C. Gao, D. Meng, Y. Yang, Y. Wang, X. Zhou, and A. G. Hauptmann, "Infrared patch-image model for small target detection in a single image," *IEEE Trans. Image Process.*, vol. 22, no. 12, pp. 4996–5009, Dec. 2013.

[17] E. J. Candès, "Robust principal component analysis?," *J. Assoc. Comput. Machinery*, vol. 58, no. 3, pp. 1–37, 2011.

[18] X. Wang, Z. Peng, D. Kong, and Y. He, "Infrared dim and small target detection based on stable multisubspace learning in heterogeneous

scene," *IEEE Trans. Geosci. Remote Sens.*, vol. 55, no. 10, pp. 5481–5493, Oct. 2017.
[19] Y. Dai and Y. Wu, "Reweighted infrared patch-tensor model with both nonlocal and local priors for single-frame small target detection," *IEEE J. Sel. Topics Appl. Earth Observ. Remote Sens.*, vol. 10, no. 8, pp. 3752–3767, Aug. 2017.
[20] L. Zhang, "Infrared small target detection via non-convex rank approximation minimization joint l 2, 1 norm," *Remote Sens.*, vol. 10, no. 11, pp. 1821, 2018.
[21] C. L. P. Chen, H. Li, Y. Wei, T. Xia, and Y. Y. Tang, "A local contrast method for small infrared target detection," *IEEE Trans. Geosci. Remote Sens.*, vol. 52, no. 1, pp. 574–581, Jan. 2014.
[22] Y. Wei, X. You, and H. Li, "Multiscale patch-based contrast measure for small infrared target detection," *Pattern Recognit.*, vol. 58, pp. 216–226, 2016.
[23] X. Bai and Y. Bi, "Derivative entropy-based contrast measure for infrared small-target detection," *IEEE Trans. Geosci. Remote Sens.*, vol. 56, no. 4, pp. 2452–2466, Apr. 2018.
[24] H. Deng, X. Sun, M. Liu, C. Ye, and X. Zhou, "Small infrared target detection based on weighted local difference measure," *IEEE Trans. Geosci. Remote Sens.*, vol. 54, no. 7, pp. 4204–4214, Jul. 2016.
[25] R. Lu, X. Yang, W. Li, J. Fan, D. Li, and X. Jing, "Robust infrared small target detection via multidirectional derivative-based weighted contrast measure," *IEEE Geosci. Remote Sens. Lett.*, vol. 19, 2022, Art. no. 7000105.
[26] Y. Shi, Y. Wei, H. Yao, D. Pan, and G. Xiao, "High-boost-based multiscale local contrast measure for infrared small target detection," *IEEE Geosci. Remote Sens. Lett.*, vol. 15, no. 1, pp. 33–37, Jan. 2018.
[27] J. Han, S. Moradi, I. Faramarzi, C. Liu, H. Zhang, and Q. Zhao, "A local contrast method for infrared small-target detection utilizing a tri-layer window," *IEEE Geosci. Remote Sens. Lett.*, vol. 17, no. 10, pp. 1822–1826, Oct. 2020.
[28] J. Han, K. Liang, B. Zhou, X. Zhu, J. Zhao, and L. Zhao, "Infrared small target detection utilizing the multiscale relative local contrast measure," *IEEE Geosci. Remote Sens. Lett.*, vol. 15, no. 4, pp. 612–616, Apr. 2018.
[29] J. Han et al., "Infrared small target detection based on the weighted strengthened local contrast measure," *IEEE Geosci. Remote Sens. Lett.*, vol. 18, no. 9, pp. 1670–1674, Sep. 2021.
[30] M. Nasiri and S. Chehresa, "Infrared small target enhancement based on variance difference," *Infrared Phys. Technol.*, vol. 82, pp. 107–119, 2017.
[31] J. MU et al., "Infrared small target detection using tri-layer template local difference measure," *Opt. Precis. Eng.*, vol. 30, no. 7, pp. 869–882, 2022.
[32] Y. Tang, K. Xiong, and C. Wang, "Fast infrared small target detection based on global contrast measure using dilate operation," *IEEE Geosci. Remote Sens. Lett.*, vol. 20, 2023, Art. no. 8000105.
[33] D. Liu, L. Cao, Z. Li, T. Liu, and P. Che, "Infrared small target detection based on flux density and direction diversity in gradient vector field," *IEEE J. Sel. Topics Appl. Earth Observ. Remote Sens.*, vol. 11, no. 7, pp. 2528–2554, Jul. 2018.
[34] B. Hui et al., "A dataset for infrared detection and tracking of dim-small aircraft targets under ground/air background," *China Sci. Data*, vol. 5, no. 3, pp. 291–302, 2020.

Dali Zhou was born in Changchun, Jilin, China, in 1989. He received the B.S. degree in electronic information science and technology and the M.S. degree in circuit and system from Northeast Normal University, Changchun, in 2013 and 2016, respectively.

He is currently an Assistant Researcher with the Changchun Institute of Optics, Fine Mechanics and Physics, Chinese Academy of Sciences, Changchun. His research interests include image processing, faint target detection, and computer vision.

Xiaodong Wang was born in Jilin, China, in 1970. He received the Ph.D. degree in optical engineering from the Changchun Institute of Optics, Fine Mechanics and Physics, Chinese Academy of Sciences, Changchun, China, in 2003.

He is currently a Researcher with the Changchun Institute of Optics, Fine Mechanics and Physics, Chinese Academy of Sciences. His research interests include space optical remote sensing imaging and information processing technology.